

# 1 RNA-Seq Time Series of *Vitis vinifera* Bud 2 Development Reveals Correlation of Expression 3 Patterns with the Local Temperature Profile

4 Boas Pucker<sup>1,3</sup>, Anna Schwandner<sup>2</sup>, Sarah Becker<sup>1</sup>, Ludger Hausmann<sup>2</sup>, Prisca Viehöver<sup>1</sup>,  
5 Reinhard Töpfer<sup>2</sup>, Bernd Weisshaar<sup>1</sup>, and Daniela Holtgräwe<sup>1,\*</sup>

6  
7 <sup>1</sup> Genetics and Genomics of Plants, Faculty of Biology and Center for Biotechnology (CeBiTec), Bielefeld  
8 University, Bielefeld, Germany; bpucker@cebitec.uni-bielefeld.de (B.P.), sabecker@techfak.uni-bielefeld.de  
9 (S.B.), viehoeve@cebitec.uni-bielefeld.de (P.V.), bernd.weisshaar@uni-bielefeld.de (B.W.),  
10 dholtgra@cebitec.uni-bielefeld.de (D.H.)

11 <sup>2</sup> Julius Kühn-Institute (JKI), Institute for Grapevine Breeding Geilweilerhof, Siebeldingen, Germany;  
12 anna.schwandner@julius-kuehn.de (A.S.), ludger.hausmann@julius-kuehn.de (L.H.),  
13 reinhard.toepfer@julius-kuehn.de (R.T.)

14 <sup>3</sup> Evolution and Diversity, Department of Plant Sciences, University of Cambridge, Cambridge, United  
15 Kingdom; bpucker@cebitec.uni-bielefeld.de (B.P.)

16 \* Correspondence: dholtgra@cebitec.uni-bielefeld.de (D.H.)  
17 ORCIDs: BP 0000-0002-3321-7471; AS 0000-0001-8755-1435; LH 0000-0002-4046-9626; RT 0000-0003-1569-  
18 2495; BW 0000-0002-7635-3473, DH 0000-0002-1062-4576.

19 Received: date; Accepted: date; Published: date

20 **Abstract:** Plants display sophisticated mechanisms to tolerate challenging environmental conditions  
21 and need to manage their ontogenesis in parallel. Here, we set out to generate an RNA-Seq time  
22 series dataset throughout grapevine (*Vitis vinifera*) early bud development. The expression of the  
23 developmental regulator *VviAP1* served as an indicator for progress of development. We  
24 investigated the impact of changing temperatures on gene expression levels during the time series  
25 and detected a correlation between increased temperatures and a high expression level of genes  
26 encoding heat-shock proteins. The data set also allowed the exemplary investigation of expression  
27 patterns of genes from three transcription factor (TF) gene families, namely MADS-box, WRKY, and  
28 R2R3-MYB genes. Inspection of the expression profiles from all three TF gene families indicated that  
29 a switch in the developmental program takes place in July which coincides with increased  
30 expression of the bud dormancy marker gene *VviDRM1*.

31

32 **Keywords:** grapevine; ontogenesis; gene expression; AP1; DRM1; MYB; WRKY; MADS-box; HSP;  
33 heat-shock genes; qRT-PCR reference genes  
34

---

## 35 1. Introduction

36 Plants are sessile organisms which cannot escape from herbivores or changes in environmental  
37 conditions. As a consequence, various stress response mechanisms [1,2] and complex specialized  
38 metabolite pathways evolved to counteract adverse situations and conditions [3,4]. These response  
39 mechanisms also need to protect plant embryogenesis, as well as vegetative developmental processes  
40 like outgrowth of side shoots from resting or latent buds. All these developmental processes,  
41 including the establishment of compound buds, have to proceed undisturbed despite potentially  
42 challenging and/or unfavorable environmental conditions.

43 Similar to other woody perennial plants like e.g. apple or poplar, *V. vinifera* (grapevine) bud  
44 development spans over two years between bud initiation and growth of new side shoots. Newly  
45 formed buds enter in a dormancy phase in the winter time between the two growing seasons before

46 buds sprout in the second season [5,6]. In spring of the first season (April/May on the northern  
47 hemisphere), new axillary buds are formed on young grapevine shoots. These new buds initially  
48 contain meristems that develop into embryonic shoots with their shoot apical meristems (SAM) and  
49 containing primordia for leaves, tendrils and inflorescences. This implies that different types of  
50 meristems, including lateral and inflorescence meristems, co-exist in the buds. Floral transition takes  
51 place at about June, five to seven weeks after burst of "old" buds (i. e. the buds that are one year ahead  
52 in development). Inflorescence primordia differentiate from uncommitted primordia formed within  
53 the new buds. Due to further differentiation of inflorescence meristems into inflorescence branch  
54 meristems (about July), the compound buds finally contain the embryonic version of next year's  
55 shoots, each with tissues for first leaves, inflorescences and tendrils [6,7]. The buds enter  
56 endodormancy which passes over into ecodormancy depending on the environmental conditions of  
57 fall and winter [8-10]. In early spring of the second season, ecodormancy is released and inflorescence  
58 branch meristems produce single flower meristems in swelling buds (April) and flower organ  
59 development begins [6]. It is important to note that the precise timing of floral transition and  
60 development strongly depend on environmental conditions and genotype.

61 Heat-shock proteins (HSPs) are a group of proteins, which were initially detected due to their  
62 accumulation in response to quickly increased temperature. They realize a molecular mechanism to  
63 endure higher temperatures. First reports of HSPs in plants reach back to the 1980s when they were  
64 described based on cell culture experiments with tobacco and soybean [11]. HSPs are assumed to  
65 support several physiological functions under normal growth conditions. This includes folding,  
66 unfolding, localization, accumulation and degradation of other proteins [12,13]. Additionally,  
67 irreversible aggregation of other proteins is prevented and refolding is facilitated under heat stress  
68 [14]. Several categories of HSPs based on sequence homology and typical molecular weight have been  
69 defined [12], thus leading to multiple polyphyletic groups of HSPs.

70 WRKY transcription factors (TFs) are a family of TFs, which play an important role in the  
71 regulation of responses to environmental stress conditions [15-17]. R2R3-MYB TFs are often  
72 responsible for controlling the formation of specialized metabolites in response to environmental  
73 triggers, but also regulate several plant-specific processes including root hair and trichome  
74 differentiation [18-20]. MADS-box TFs are typically involved in the regulation of developmental  
75 processes like determination of plant organ identity [21-23]. One especially important developmental  
76 regulator is APETALA1 (AP1), also a MADS-box factor, which connects signals received from the  
77 environment with initiation and/or progress of developmental processes [24,25]. *VviAP1* and  
78 *VviAIL2*, a *V. vinifera* homolog of the MADS-box gene *AINTEGUMENTA-like* (*AtAIL1*, At1g72570),  
79 have been postulated to be involved in the photoperiodic control of seasonal growth [26]. In addition,  
80 marker genes for the dormant state of buds have been described. One such marker gene is *DRM1*, a  
81 gene that has been found initially in *Pisum sativum* to encode a dormancy-associated protein [27].  
82 Subsequently, *DRM1* homologs have been identified in many species in the context of bud dormancy,  
83 including *V. vinifera* [10,28].

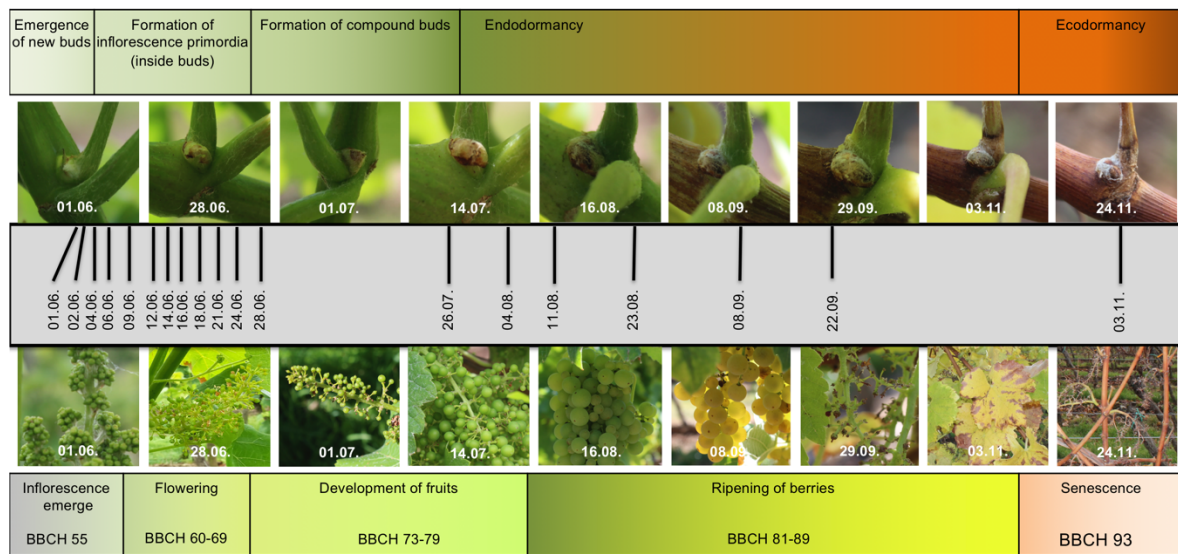
84 In the model plant *Arabidopsis thaliana*, phylotranscriptomic evidence for a molecular embryonic  
85 hourglass was published [29-31]. We attempted to create an RNA-Seq dataset to examine early bud  
86 development of *V. vinifera* for a similar general pattern. While an hourglass pattern was not detected  
87 in the data (M. Quint, personal communication), we harnessed the time series of *V. vinifera* RNA-Seq  
88 samples to investigate changes in gene expression during early bud development throughout the first  
89 season at a fine scale and observed a strong influence of high temperatures on the expression of HSP  
90 genes of field grown plants. In addition, a switch in the expression patterns of various TF genes was  
91 observed that happens in parallel to or shortly after the switch from uncommitted primordia to  
92 inflorescence primordia. This switch in expression pattern coincides with onset of expression of the  
93 dormancy marker gene *VviDRM1*.

94

## 95 2. Results

96 2.1. RNA-Seq Time Series of Early Bud Development and Transcript Accumulation Patterns of Selected  
97 Marker Genes

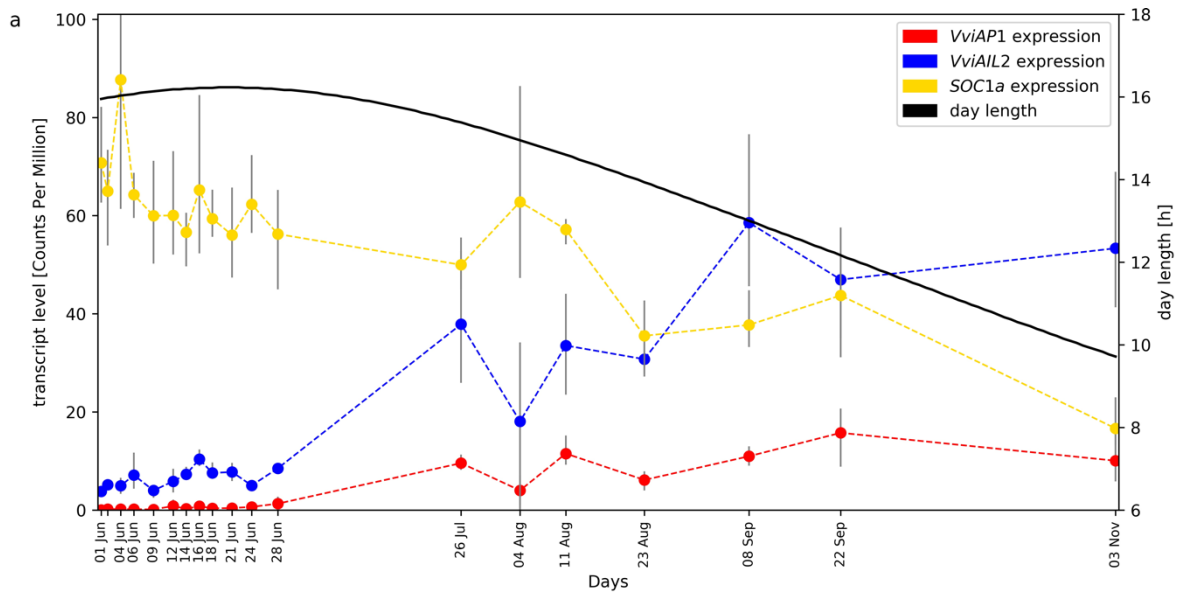
98 Young buds of *V. vinifera* 'Calardis Musqué' were harvested in a vineyard in the south of  
99 Germany over a period of 156 days of the first season of development, covering the time from June  
100 1st to November 3rd of 2016 (Figure 1) (File S1). Per time point, buds derived from three vines were  
101 harvested and subjected to RNA-Seq analyses in triplicates per time point. Values for gene  
102 expression, inferred from values for transcript accumulation, were calculated for all transcribed  
103 genes. (File S2, File S3, File S4; see methods for details). Time points with only two successful  
104 biological replicates were included in the submission to the European Nucleotide Archive (ENA)  
105 database (File S1), but excluded from the investigations presented here.  
106



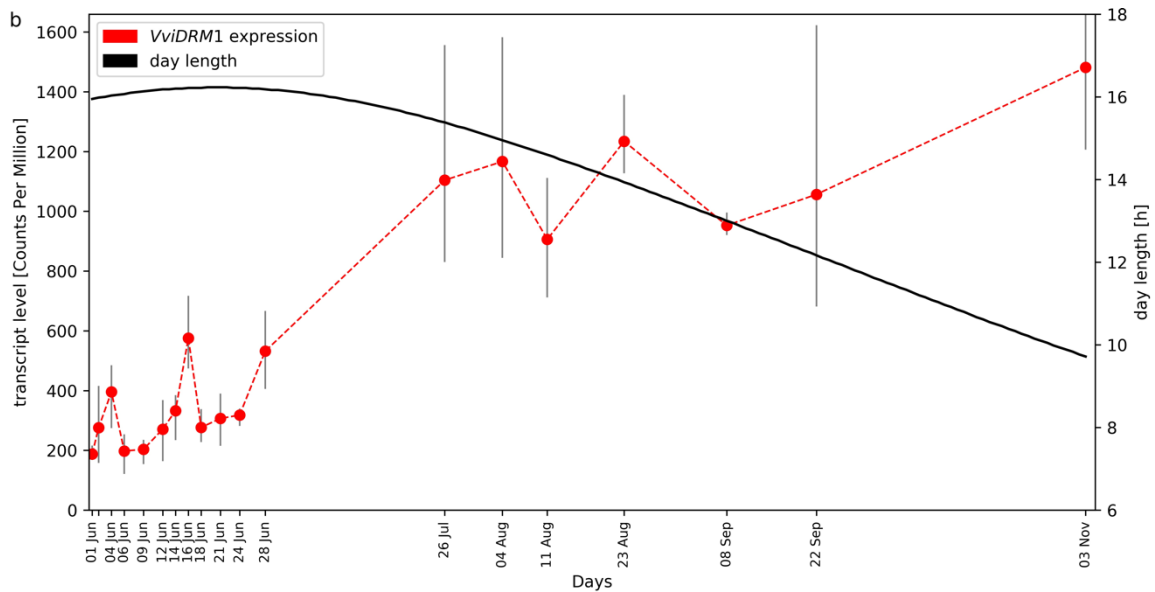
107  
108 **Figure 1.** Documentation of the grapevine material used for sampling. The upper row of pictures displays the  
109 bud stages during the first year of development, which were the target of this study. The lower row of pictures  
110 displays the growth status of the vines from which the young buds were taken. In the center (grey bar), the  
111 sampling time line is depicted.

112 The expression pattern of the MADS-Box genes *VviAP1* (CRIBI2.1 ID VIT\_201s0011g00100),  
113 *VviAIL2* (VIT\_209s0002g01370), and *VviSOC1a* (VIT\_215s0048g01250) are displayed in Figure 2a.  
114 *VviAP1* transcript levels were zero or very low until end of June and rise until September. Due to the  
115 time distance between the sampling points we interpret the data as essentially one peak in September.  
116 *VviAP1* and *VviAIL2* display quite similar expression patterns. The increase of *VviAP1* transcript  
117 levels at the end of June correlates with the time when floral transition, the differentiation of  
118 uncommitted primordia into inflorescence primordia, took place. There is no direct correlation  
119 between the transcript levels of *VviAP1* and *VviAIL2* with the day length, but the rise of transcript  
120 levels coincides with the beginning of reduction of day length after midsummer. We also checked the  
121 expression of the dormancy marker gene *VviDRM1* (VIT\_210s0003g00090) and found high transcript  
122 levels of this gene in the buds with a clear increase starting in July (Figure 2b).

123



124



125

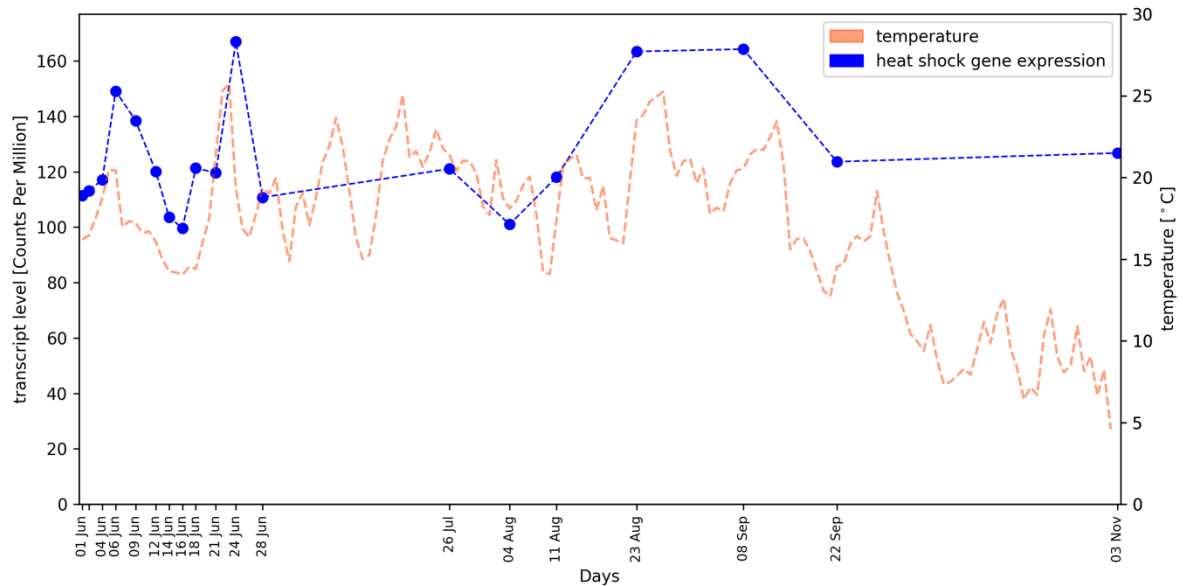
126 **Figure 2:** Gene expression time course of *VviAP1*, *VviAIL2*, and *SOC1a* (panel a) as well as *VviDRM1*  
127 (panel b) in developing grapevine buds. The plots were separated due to the large difference in  
128 transcript levels (detected as standardized read counts), see y-axis on the left. Day length during the  
129 sampling interval is plotted in both panels.

130

## 131 2.2. Average Gene Expression Values of HSP Genes Reflect the Local Temperature Profile

132 We made use of the weather data recorded at the vineyard from which the samples for RNA-  
133 Seq were derived. Since the recorded temperature profile during 2016 displayed significant  
134 oscillation, we tested the hypothesis that a heat-shock response may take place in the buds. A total of  
135 131 putative HSP genes were identified based on the annotation (File S5), but only 80 of these show  
136 substantial transcript abundance (CPM value of more than 10). The gene expression pattern of this  
137 set of 80 HSP genes shows a good correlation ( $r \approx 0.45$ ) with the temperature profile. Obviously, the  
138 correlation is much better during the period with dense sampling. We observed clear HSP gene  
139 transcript level peaks at time points with high temperatures (Figure 3). This is especially noticeable

140 at June 24th when the highest average temperature was recorded. A correlation of the day  
141 length/photoperiod with the expression pattern of these genes was not observed.  
142



143

144 **Figure 3:** Correlation of HSP gene expression (blue dots / blue dotted line) in developing grapevine  
145 buds and environmental air temperature (red dashed line); the course of the daily average  
146 temperature values is shown.

### 147 2.3. Investigation of Transcription Factor Gene Families: WKRY, MADS-box, and R2R3-MYBs

148 We harnessed the presented RNA-Seq time series for the analyses of expression patterns of three  
149 TF gene families. Heatmaps display transcript levels of genes encoding MADS-box (File S6), R2R3-  
150 MYB (File S7), and WRKY (File S8) TFs. Only genes that display detectable transcript accumulation  
151 values were considered (see Methods for the threshold). As can be seen from all three heatmaps, the  
152 gene activity patterns of quite some of the transcription factor genes change quite dramatically with  
153 the onset of *VviAP1* transcript accumulation between June 28th and July 26th.

154 While *VviSVP1* (VIT\_200s0313g00070), an ortholog of the *A. thaliana* MADS-box gene *SHORT*  
155 *VEGETATIVE PHASE/AGL22* (At2g22540), shows transcript levels with almost constant values, the  
156 gene *VviFLC2* (VIT\_214s0068g01800) displays a time course quite similar to those of *VviAP1* and  
157 *VviAIL2*. *VviFLC2* is, like its paralog *VviFLC1* (VIT\_201s0010g03890), closely related to the *A. thaliana*  
158 MADS box gene *FLOWERING LOCUS C/AGL25* (At5g10140) which encodes a central repressor of the  
159 floral transition. In contrast, *VviTM8a* (VIT\_217s0000g01230), which was named according to a gene  
160 initially detected in *Solanum lycopersicum* (*TOMATO MADS 8*) that became "founder" of a specific  
161 sub-clade of evolutionary related MADS-box genes, shows a transcript accumulation peak at the end  
162 of June. Finally, *VviSOC1a* (VIT\_215s0048g01250), a homolog of the *A. thaliana* MADS box gene  
163 *SUPPRESSOR OF OVEREXPRESSION OF CO 1/AGL20* (At2g45660) displays transcript  
164 accumulation values that decline after middle of August (Figure 2a).

165 With regard to the R2R3-MYB genes, *VviMYBC2-L1* (VIT\_201s0011g04760), *VviMYB4A*  
166 (VIT\_203s0038g02310), and *VviMYBPAR* (VIT\_211s0016g01300) are prominent examples of genes  
167 that support the gene expression pattern switch during July. In addition to the July switch, several  
168 R2R3-MYB genes display high transcript accumulation values specifically in November. Clear  
169 examples are *VviMYB15* (VIT\_205s0049g01020), *VviMYB14* (VIT\_205s0049g01020), and *VviMYB30A*  
170 (VIT\_217s0000g06190). Based on its high transcript levels, *VviMYBPA1* (VIT\_215s0046g00170), a  
171 homolog of the *A. thaliana* R2R3-MYB genes *TRANSPARENT TESTA 2/AtMYB123* (At5g35550) and  
172 *AtMYB5* (At3g13540), appears as an important regulator. It is worth noting that another homolog of  
173 *AtMYB123* and *AtMYB5*, namely *VviMYBPAR*, also shows high transcript levels from end of August  
174 to September. Another R2R3-MYB gene that stands out due to high transcript levels is *VviMYB174*

175 (VIT\_218s0001g09850), a homolog of *AtMYB73* (At4g37260) and *AtMYB77* (At3g50060). As expected  
176 for organs/tissue not accumulating anthocyanins, *VviMYBA1* (VIT\_202s0033g00410), an ortholog of  
177 the *A. thaliana* R2R3-MYB gene *PRODUCTION OF ANTHOCYANIN PIGMENT 1/AtMYB75*  
178 (At1g56650), is not significantly expressed in young buds.

179 Several genes encoding TFs of the WRKY type show a substantial increase of transcript levels at  
180 the gene expression pattern switch during July (e.g. *VviWRKY20* (VIT\_207s0005g02570) or  
181 *VviWRKY31* (VIT\_210s0003g02810)). Examples for the opposite change, i.e. reduction of transcript  
182 levels during July, are *VvWRKY23* (VIT\_207s0031g01840) and *VviWRKY41* (VIT\_213s0067g03140).  
183 High transcript levels that are strongly reduced towards winter were detected for *VviWRKY25*  
184 (VIT\_208s0058g01390) that is, together with *VviWRKY41*, homologous to *AtWRKY54* (At2g40750),  
185 *AtWRKY70* (At3g56400) and *AtWRKY46* (At2g46400). Like some of the R2R3-MYB genes, also several  
186 *VviWRKY* genes display high transcript accumulation values specifically in November and/or an  
187 increase towards winter. These include *VviWRKY16* (VIT\_206s0004g07500), *VviWRKY45*  
188 (VIT\_214s0108g01280) and *VviWRKY33* (VIT\_211s0037g00150) that are all homologous to the *A.*  
189 *thaliana* WRKY genes of group I-C including *AtWRKY33* (At2g38470), *AtWRKY58* (At3g01080), and  
190 *AtWRKY32* (At4g30935).

#### 191 2.4. Identification of qRT-PCR Reference Genes

192 The quite long RNA-seq time series from tissue of compound buds, covering changing day  
193 length and oscillating weather conditions in the field, allowed the identification of candidate  
194 reference genes for quantitative Real-Time PCR (qRT-PCR) experiments. The 20 best candidates for  
195 reference genes in qRT-PCR experiments were predicted based on an overall high expression and a  
196 low variation in steady-state transcript abundance (File S9). A manual inspection of the functional  
197 annotation of these genes supported the quality of this data set since it covers well-known qRT-PCR  
198 reference genes like 'polyubiquitin', 'glyceraldehyde-3-phosphate dehydrogenase', 'elongation factor  
199 Tu', and 'actin' as top candidates. The most promising candidate is *VviUBQ10* (VIT\_219s0177g00040)  
200 which is homologous to the five *A. thaliana* genes encoding polyubiquitin (At4g05320 and others).  
201 The second best candidate is VIT\_219s0015g01090, a homolog of *A. thaliana* *HEAT SHOCK PROTEIN*  
202 *81.4* (At5g56000).

### 203 3. Discussion

204 This time series of 18 RNA-Seq data points throughout the first year of development of *V. vinifera*  
205 compound buds allows the investigation of developmental processes at relatively high resolution. A  
206 similar time series analyses has been performed previously with Affymetrix arrays to determine gene  
207 expression patterns for the cultivar Tempranillo [9]. While the data from Tempranillo that was grown  
208 near Madrid cover the time from May (first year) to April (second year) with 8 time points, the focus  
209 of the time series presented here was the early bud development in June until November of the first  
210 year. Nevertheless, the previously reported expression pattern changes in July and also towards  
211 winter (November time point) [9] were essentially matched by our data set.

212 Our chronologically dense collection of samples allows the detection of small developmental  
213 differences between time points, but it is affected by a high variation through individual differences  
214 between plants, sampled buds, and varying environmental conditions like temperature and other  
215 weather conditions. Harvesting the buds in the field is technically challenging since the buds are  
216 small and need to be cut out of the axil between shoot and leaf or from hard wood. The sampling  
217 has to be performed quickly and there was no time to remove adhering tissue from shoots before  
218 freezing the samples in liquid nitrogen. The results presented were derived from data of the year  
219 2016 and from time points for which three independent biological replicates were available.  
220 However, there are more data of time points for which individual replicates were lost mainly during  
221 the RNA extraction procedures due to the problematic technical properties of the respective samples  
222 (File S1). While these time points should not be used for statistical analyses, they still provide  
223 additional support for patterns observed or may increase the power of co-expression analyses in the  
224 future.

225 Predicted reference genes for qRT-PCR experiments of bud samples contain commonly used  
226 reference genes like GAPDH, actin, polyubiquitin, and elongation factor Tu. Additionally, novel  
227 candidate genes were identified which displayed a constant expression level. This aligns well with a  
228 previous study, which reported that novel reference genes identified by genome-wide *in silico*  
229 analysis outperformed typical reference genes in common wheat [32].

230 We selected three well-known and in the model plant *A. thaliana* well-characterised TF gene  
231 families for more detailed analyses of gene expression patterns. MADS-box genes were selected  
232 because of their relation to development, and also because quite some of these genes were analysed  
233 in the Tempranillo study of Diaz-Riquelme et al. [9]. R2R3-MYB genes and WRKY genes were  
234 selected because of their link to stress responses as well as control of accumulation of specialized  
235 metabolites.

236 The gene *VviSOC1a*, a potential integrator of multiple flowering signals that cumulate in the  
237 establishment of inflorescence meristems [33], is expressed in June and expression declines after  
238 middle of August, when *VviAP1* and also *VviLFY/VviFL* (VIT\_217s0000g00150, see File S3; ortholog  
239 of *AtLEAFY* [34], At5g61850) show increasing expression levels. This increased expression of  
240 potential inflorescence meristem identity genes (*AP1*, *LEAFY*) coincides with proliferation of  
241 inflorescence primordia, giving rise to inflorescence branch primordia in the developing compound  
242 buds [5,6,35]. Based on the also increasing expression of the dormancy marker gene *VviDRM1*, it can  
243 be postulated that other parts of the compound bud are already in July on their way to  
244 endodormancy. Also the gene *VviTM8a*, a homolog of *TOMATO MADS 8* that plays a role in tomato  
245 flower development [36], displays an interesting expression pattern that hints at inflorescence  
246 developmental processes taking place during June and beginning of July.

247 With respect to the expression of the two R2R3-MYB factors known to control proanthocyanidin  
248 (PA) biosynthesis that displayed conspicuous expression patterns, namely *VviMYBPA1* and  
249 *VviMYBPAR* [37,38], three prominent potential target genes *VviLAR1* (VIT\_201s0011g02960) *VviANS*  
250 (or *VviLDOX*, VIT\_202s0025g04720) and *VviANR* (VIT\_200s0361g00040) show expression patterns  
251 expected for targets (File S3), also with a reduction of expression levels towards winter. The three  
252 genes encode the enzymes leucoanthocyanidin reductase (LAR), anthocyanidin synthase (ANS, also  
253 referred to as LDOX) and anthocyanidin reductase (ANR) which are required for biosynthesis of  
254 catechin and epicatechin that are precursors of PAs [38]. This indicates that the compound buds  
255 accumulate PAs during summer and fall in preparation for winter. Similarly, it is conceivable that  
256 the activation of *VviMYB14* and *VviMYB15* results in the synthesis of stilbenes [39,40], which fits to  
257 the activation of three of the *V. vinifera* stilbene synthase genes [41] that are clustered on chromosome  
258 16. While *VviSTS35* (VIT\_216s0100g01070) and *VviSTS41* (VIT\_216s0100g01130) might be targets of  
259 *VviMYB15* based on strong co-expression in November, *VviSTS36* (VIT\_216s0100g01100) fits better  
260 as a potential target of *VviMYB14*. The analysis of *VviSTS* genes [41] also covered three *VviCHS* genes  
261 (*VviCHS3*: VIT\_205s0136g00260, *VviCHS1*: VIT\_214s0068g00920 and *VviCHS2*: VIT\_214s0068g00930).  
262 The three *VviCHS* genes are co-expressed with a pattern similar to that of *VviLAR1*, *VviANS* and  
263 *VviANR* which fits the substrate requirement for catechin/epicatechin biosynthesis and to  
264 *VviMYBPA1* and/or *VviMYBPAR* as potential regulators. The homologs of the highly expressed gene  
265 *VviMYB174*, *AtMYB73* and *AtMYB77*, have been implicated in root-related auxin responses [42]. A  
266 similar function of *VviMYB174* would fit to its high expression throughout compound but  
267 development from June to November.

268 Of the *VviWRKY* genes that have been implicated in the control of *VviSTS*'s, namely *VviWRKY03*,  
269 *VviWRKY24*, *VviWRKY43* and *VviWRKY53* [40], only *VviWRKY03* (VIT\_201s0010g03930) displayed  
270 expression with a pattern that fits to that of *VviMYB14* and *VviSTS36*, allowing to hypothesize that  
271 *STS36* expression is under combinatorial control of *MYB14*/*WRKY03* in compound buds.  
272 *VviWRKY25*, and to some extent *VviWRKY41* as well, that are both homologous to the *AtWRKY* genes  
273 implicated in brassinosteroid-regulated plant growth [43], show expression patterns that fit to growth  
274 actions until September that are then abandoned towards November and winter.

275 To the best of our knowledge, this is the first report of a correlation between HSP gene expression  
276 patterns with the environmental temperature in a comprehensive time series of field (vineyard)

277 samples. However, repeated formation of HSPs was previously described in the seeds, seed pods,  
278 and flowers of *Medicago sativa* [44]. The occurrence of HSPs at standard (not stressed) growth  
279 conditions indicated a potential role in development [44]. The annotation “heat-shock” was initially  
280 introduced based on up-regulation of genes in heat stress experiments [11,45]. HSPs were also  
281 detected at substantial levels in field-grown *Gossypium hirsutum* under increased temperature and  
282 drought stress [46]. Reports from *Oryza sativa* support the stress signal integration function of HSPs  
283 [47]. Therefore, we also checked for other stress factors like documented pathogen attack, crop  
284 protection treatments, or drought stress, but temperature was the only factor with a substantial  
285 correlation. Considering the large number of physiological functions of HSPs, constantly expressed  
286 chaperons might also be annotated as HSPs. The observation of constant high expression for a gene  
287 annotated as “heat-shock protein” (VIT\_219s0015g01090) among the potential reference genes for  
288 qRT-PCR supports this hypothesis. This assumption aligns well with previous findings that HSPs  
289 can have functions in the integration of stress signals [48]. Since our analysis of HSPs is based on the  
290 currently available functional annotation, it is likely that the gene expression correlation of bona fide  
291 HSP genes with the temperature profile might be even stronger than described here. Moreover, it is  
292 possible that additional factors like an underlying developmental pattern or UV-B exposure have an  
293 additional influence on the observed heat-shock gene expression profile.  
294

## 295 4. Materials and Methods

### 296 4.1. Biological Material

297 Buds of consecutive time points within the first year of their developmental cycle were taken  
298 from a vineyard of the cultivar ‘Calardis Musqué’ (‘Bacchus Weiss’ x ‘Seyval’), former breeding line  
299 GF.GA-47-42 (VIVC variety number 4549; <http://www.vivc.de>). The plot consists of 1300 vines,  
300 planted in 1995, pruned as a single cane Guyot system, and located at the Institute for Grapevine  
301 Breeding Geilweilerhof in Siebeldingen (49°13'05.0"N 8°02'45.0"E), about 120 m north of a weather  
302 station (<https://www.am.rlp.de/Internet/AM/NotesAM.nsf/amwebagrar/>). Early in the afternoon on  
303 each sampling date of the growing season, bud samples were taken in triplicates. From three different  
304 vines four buds each were harvested in a batch and immediately frozen in liquid nitrogen. The buds  
305 were taken from the fourth to eight node of the shoots emerging from the middle section of the cane  
306 (Figure 4). Vines that appeared to be equal in their overall developmental stage were chosen. Those  
307 that showed symptoms of nutrient deficiency or diseases were excluded as a sample source.



308  
309 **Figure 4:** The same vine of ‘Calardis Musqué’ on 1st of July and 16th of December 2016. White circles mark the  
310 fourth to eighth node of the middle shoots from which the buds were harvested.

### 311 4.2. RNA Extraction, Library Preparation, and Sequencing



312 Total RNA was extracted, from four buds each, in triplicate per time point. Up to 100 mg of  
313 liquid nitrogen ground tissue was applied to the Spectrum™ Plant Total RNA kit (Sigma-Aldrich,  
314 Taufkirchen, Germany) according to the manufacturer's instructions for protocol B. After on-column  
315 DNase treatment with the DNase I Digest Set (Sigma-Aldrich, Taufkirchen, Germany), the RNA was  
316 quantified. 500 ng total RNA per sample were used to prepare sequencing libraries according to the  
317 Illumina TruSeq RNA Sample Preparation v2 Guide. Purification of the polyA-containing mRNA  
318 was performed using two rounds of oligo(dT) oligonucleotides attached to magnetic beads. During  
319 the second elution of the polyA+ RNA, the RNA was fragmented and primed for cDNA synthesis.  
320 After cDNA synthesis, the DNA fragments were end-repaired and A-tailing was performed. Multiple  
321 indexing adapters, specific for each library and sample, were ligated to the ends of the cDNA  
322 fragments and the adapter ligated fragments were enriched by 12 cycles of PCR. After qualification  
323 and quantification, the resulting sequencing libraries were equimolarly pooled and sequenced  
324 generating 100 nt single-end reads on eight lanes of an Illumina HiSeq1500 flowcell at the Sequencing  
325 Core Facility of the Center for Biotechnology (CeBiTec) at Bielefeld University.

#### 326 4.3. Bioinformatic Analysis of RNA-Seq Data

327 All RNA-Seq read data sets generated were submitted to the ENA (for accession numbers see  
328 File S1). Python scripts developed for customized analyses are available at Github:  
329 <https://github.com/bpucker/vivi-bud-dev>. RNA-Seq reads were mapped to the CRIBI2.1 reference  
330 genome sequence of PN40024 [49] via STAR v.2.51b [50] with previously optimized parameters  
331 including a minimal alignment length cutoff of 90% and a minimal similarity cutoff of 95% of the  
332 read length [51]. FeatureCounts [52] was deployed for quantification of steady-state transcript levels  
333 at the gene level based on these mappings and the CRIBI2.1 annotation [53]. Previously developed  
334 Python scripts [51] were applied to merge the resulting count tables and to calculate counts per  
335 million (CPMs) and reads per kb per million mapped reads (RPKMs). We attempted to include *VviFT*  
336 (GSVIVT00012870001 in the Vv8x genome sequence) in the analyses of selected target genes, but the  
337 corresponding sequence region is not included in the genome sequence version (file Vv12x\_CRIBI.fa)  
338 on which the CRIBI2.1 annotation is based. To include the three *VviCHS* genes [41], structural gene  
339 annotation was optimised for VIT\_214s0068g00920 and VIT\_214s0068g00930.

340 Average day temperature values were retrieved from the weather station in the vineyard for the  
341 time from June 1st to November 3rd of 2016.

342 HSP genes in CRIBI2.1 were identified based on the annotation text of homologs in *A. thaliana*  
343 by filtering for the strings 'heat' and 'shock' occurring together in the functional annotation text of  
344 the genes. Lowly expressed genes were excluded from downstream analyses by applying a minimal  
345 CPM cutoff of 10 (per gene sum over all samples). The Python package matplotlib v2.1.0 [54] was  
346 used for visualization of the data.

347 Members of the transcription factor families WRKY [16], MADS-box [23], and MYB [19,39] were  
348 identified based on the published gene family analyses. The *V. vinifera* WRKY gene family has also  
349 been characterised by Guo et al. (2014) [55] which, unfortunately, resulted in conflicting gene  
350 designations. For consistency with Vannozzi et al. [40] we only used the *VviWRKY* gene designations  
351 of Wang et al. (2014). To allow the expression analysis of all previously described MADS-box genes,  
352 the CRIBI v2.1 annotation was extended with corresponding gene models using "VIT\_230\_" as prefix  
353 for the additional locus IDs. The Python packages matplotlib v2.1.0 [54] and seaborn v0.8.1  
354 (<https://github.com/mwaskom/seaborn>) were used for visualization of RPKM values of selected  
355 genes in heatmaps.

356 Candidates for reference genes suitable for qRT-PCR experiments in the future were identified  
357 based on our comprehensive set of RNA-Seq samples. First, genes with a substantial expression level  
358 defined as sum of all samples greater or equal to 500 [CPM] were selected. Second, these candidate  
359 set was filtered for a low variation defined as small standard deviation values across all samples  
360 normalized by the median of all values.

361

362 **Supplementary Materials:** The following files are available online at [www.mdpi.com/xxx/s1](http://www.mdpi.com/xxx/s1):  
363 File S1: RNA-Seq sample overview including ENA accessions and number of reads per sample,  
364 File S2: Raw counts of RNA-Seq reads mapped to CRIBI2.1,  
365 File S3: CPMs of RNA-Seq reads mapped to CRIBI2.1,  
366 File S4: RPKMs of RNA-Seq reads mapped to CRIBI2.1,  
367 File S5: IDs of potential heatshock genes in CRIBI2.1,  
368 File S6: Gene expression heatmap of genes encoding MADS-box TFs,  
369 File S7: Gene expression heatmap of genes encoding R2R3-MYB TFs,  
370 File S8: Gene expression heatmap of genes encoding WRKY TFs,  
371 File S9: List of candidates for qRT-PCR reference genes.  
372

373 **Author Contributions:** DH, LH, RT and BW conceived and designed research. BP, AS, SB, and PV conducted  
374 the experiments. BP, LH, DH and BW interpreted the data. BP, DH, and BW wrote the manuscript. All authors  
375 read and approved the final version of the manuscript.

376

377 **Funding:** We acknowledge the financial support of the German Research Foundation (DFG, <http://www.dfg.de>)  
378 to BW (WE1576/16-2) and to RT (TO152/5-2) in the context of SPP-1530. In addition, this paper is also based on  
379 work from COST Action CA 17111 INTEGRAPPE, supported by COST (European Cooperation in Science and  
380 Technology).

381 **Acknowledgments:** We are grateful to Willy Keller for excellent technical assistance. In addition, the authors  
382 wish to thank all members of the group "Genetics and Genomics of Plants" and the Bioinformatics Resource  
383 Facility of the CeBiTec for their excellent assistance and support. We also acknowledge the financial support of  
384 the German Research Foundation and the Open Access Publication Fund of Bielefeld University for the article  
385 processing charge.

386 **Conflicts of Interest:** The authors declare no conflict of interest.

387

## 388 References

- 389 1. Bokszczanin, K.L.; Solanaceae Pollen Thermotolerance Initial Training Network, C.; Fragkostefanakis, S.  
390 Perspectives on deciphering mechanisms underlying plant heat stress response and thermotolerance.  
391 *Frontiers in Plant Science* 2013, 4, 315, doi:10.3389/fpls.2013.00315.
- 392 2. Basu, S.; Ramegowda, V.; Kumar, A.; Pereira, A. Plant adaptation to drought stress. *F1000Research* 2016, 5,  
393 1554, doi:10.12688/f1000research.7678.1.
- 394 3. Caretto, S.; Linsalata, V.; Colella, G.; Mita, G.; Lattanzio, V. Carbon Fluxes between Primary Metabolism  
395 and Phenolic Pathway in Plant Tissues under Stress. *International Journal of Molecular Sciences* 2015, 16,  
396 26378-26394, doi:10.3390/ijms161125967.
- 397 4. Yang, L.; Wen, K.S.; Ruan, X.; Zhao, Y.X.; Wei, F.; Wang, Q. Response of Plant Secondary Metabolites to  
398 Environmental Factors. *Molecules* 2018, 23, doi:10.3390/molecules23040762.
- 399 5. Carmona, M.J.; Chaïb, J.; Martínez-Zapater, J.M.; Thomas, M.R. A molecular genetic perspective of  
400 reproductive development in grapevine. *Journal of Experimental Botany* 2008, 59, 2579-2596,  
401 doi:10.1093/jxb/ern160.
- 402 6. Vasconcelos, C.M.; Greven, M.; Winefield, C.S.; Trought, M.C.T.; Raw, V. The Flowering Process of *Vitis*  
403 *vinifera*: A Review. *American Journal of Enology and Viticulture* 2009, 60, 411-434.
- 404 7. May, P. From bud to berry, with special reference to inflorescence and bunch morphology in *Vitis vinifera*  
405 L. *Australian Journal of Grape and Wine Research* 2000, 6, 82-98, doi:10.1111/j.1755-0238.2000.tb00166.x.
- 406 8. Rohde, A.; Bhalerao, R.P. Plant dormancy in the perennial context. *Trends in Plant Science* 2007, 12, 217-  
407 223, doi:10.1016/j.tplants.2007.03.012.
- 408 9. Diaz-Riquelme, J.; Grimplet, J.; Martínez-Zapater, J.M.; Carmona, M.J. Transcriptome variation along bud  
409 development in grapevine (*Vitis vinifera* L.). *BMC Plant Biology* 2012, 12.
- 410 10. Tarancon, C.; Gonzalez-Grandio, E.; Oliveros, J.C.; Nicolas, M.; Cubas, P. A Conserved Carbon Starvation  
411 Response Underlies Bud Dormancy in Woody and Herbaceous Species. *Frontiers in Plant Science* 2017, 8,  
412 788, doi:10.3389/fpls.2017.00788.

- 413 11. Barnett, T.; Altschuler, M.; McDaniel, C.N.; Mascarenhas, J.P. Heat shock induced proteins in plant cells.  
414 *Developmental Genetics* 1980, 1, 331-340, doi:10.1002/dvg.1020010406.
- 415 12. Feder, M.E.; Hofmann, G.E. Heat-shock proteins, molecular chaperones, and the stress response:  
416 evolutionary and ecological physiology. *Annual Review Physiology* 1999, 61, 243-282,  
417 doi:10.1146/annurev.physiol.61.1.243.
- 418 13. Gupta, S.C.; Sharma, A.; Mishra, M.; Mishra, R.K.; Chowdhuri, D.K. Heat shock proteins in toxicology: how  
419 close and how far? *Life Sciences* 2010, 86, 377-384, doi:10.1016/j.lfs.2009.12.015.
- 420 14. Tripp, J.; Mishra, S.K.; Scharf, K.D. Functional dissection of the cytosolic chaperone network in tomato  
421 mesophyll protoplasts. *Plant, Cell and Environment* 2009, 32, 123-133, doi:10.1111/j.1365-3040.2008.01902.x.
- 422 15. Rushton, P.J.; Somssich, I.E.; Ringler, P.; Shen, Q.J. WRKY transcription factors. *Trends in Plant Science*  
423 2010, 15, 247-258, doi:10.1016/j.tplants.2010.02.006.
- 424 16. Wang, M.; Vannozzi, A.; Wang, G.; Liang, Y.H.; Tornielli, G.B.; Zenoni, S.; Cavallini, E.; Pezzotti, M.; Cheng,  
425 Z.M. Genome and transcriptome analysis of the grapevine (*Vitis vinifera* L.) WRKY gene family.  
426 *Horticulture Research* 2014, 1, 14016, doi:10.1038/hortres.2014.16.
- 427 17. Jiang, J.; Ma, S.; Ye, N.; Jiang, M.; Cao, J.; Zhang, J. WRKY transcription factors in plant responses to stresses.  
428 *Journal of Integrative Plant Biology* 2017, 59, 86-101, doi:10.1111/jipb.12513.
- 429 18. Dubos, C.; Stracke, R.; Grotewold, E.; Weisshaar, B.; Martin, C.; Lepiniec, L. MYB transcription factors in  
430 *Arabidopsis*. *Trends in Plant Science* 2010, 15, 573-581, doi:10.1016/j.tplants.2010.06.005.
- 431 19. Matus, J.T.; Aquea, F.; Arce-Johnson, P. Analysis of the grape MYB R2R3 subfamily reveals expanded wine  
432 quality-related clades and conserved gene structure organization across *Vitis* and *Arabidopsis* genomes.  
433 *BMC Plant Biology* 2008, 8, 83, doi:10.1186/1471-2229-8-83.
- 434 20. Baldoni, E.; Genga, A.; Cominelli, E. Plant MYB Transcription Factors: Their Role in Drought Response  
435 Mechanisms. *Int J Mol Sci* 2015, 16, 15811-15851, doi:10.3390/ijms160715811.
- 436 21. Masiero, S.; Colombo, L.; Grini, P.E.; Schnittger, A.; Kater, M.M. The emerging importance of type I MADS  
437 box transcription factors for plant reproduction. *The Plant Cell* 2011, 23, 865-872,  
438 doi:10.1105/tpc.110.081737.
- 439 22. Horvath, D.P. Dormancy-Associated MADS-BOX Genes: A Review. In *Advances in Plant Dormancy*,  
440 Anderson, J.V., Ed. 2015; 10.1007/978-3-319-14451-1\_7pp. 137-146.
- 441 23. Grimplet, J.; Martínez-Zapater, J.M.; Carmona, M.J. Structural and functional annotation of the MADS-box  
442 transcription factor family in grapevine. *BMC Genomics* 2016, 17, 80, doi:10.1186/s12864-016-2398-7.
- 443 24. Wagner, D.; Sablowski, R.W.; Meyerowitz, E.M. Transcriptional activation of APETALA1 by LEAFY.  
444 *Science* 1999, 285, 582-584, doi:10.1126/science.285.5427.582.
- 445 25. Kaufmann, K.; Wellmer, F.; Muino, J.M.; Ferrier, T.; Wuest, S.E.; Kumar, V.; Serrano-Mislata, A.; Madueno,  
446 F.; Krajewski, P.; Meyerowitz, E.M., et al. Orchestration of floral initiation by APETALA1. *Science* 2010,  
447 328, 85-89, doi:10.1126/science.1185244.
- 448 26. Vergara, R.; Noriega, X.; Parada, F.; Dantas, D.; Perez, F.J. Relationship between endodormancy,  
449 FLOWERING LOCUS T and cell cycle genes in *Vitis vinifera*. *Planta* 2016, 243, 411-419, doi:10.1007/s00425-  
450 015-2415-0.
- 451 27. Stafstrom, J.P.; Ripley, B.D.; Devitt, M.L.; Drake, B. Dormancy-associated gene expression in pea axillary  
452 buds. Cloning and expression of PsDRM1 and PsDRM2. *Planta* 1998, 205, 547-552,  
453 doi:10.1007/s004250050354.
- 454 28. Zhu, Y.; Wagner, D. Plant Inflorescence Architecture: The Formation, Activity, and Fate of Axillary  
455 Meristems. *Cold Spring Harbor Perspectives in Biology* 2020, 12, a034652, doi:10.1101/cshperspect.a034652.
- 456 29. Quint, M.; Drost, H.G.; Gabel, A.; Ullrich, K.K.; Bönn, M.; Grosse, I. A transcriptomic hourglass in plant  
457 embryogenesis. *Nature* 2012, 490, 98-101.
- 458 30. Drost, H.G.; Bellstädt, J.; Ó'Maoiléidigh, D.S.; Silva, A.T.; Gabel, A.; Weinholdt, C.; Ryan, P.T.; Dekkers, B.J.;  
459 Bentsink, L.; Hillhorst, H.W., et al. Post-embryonic Hourglass Patterns Mark Ontogenetic Transitions in  
460 Plant Development. *Molecular Biology and Evolution* 2016, 33, 1158-1163.
- 461 31. Drost, H.G.; Janitza, P.; Grosse, I.; Quint, M. Cross-kingdom comparison of the developmental hourglass.  
462 *Current Opinion in Genetics & Development* 2017, 45, 69-75.
- 463 32. Dudziak, K.; Sozoniuk, M.; Szczerba, H.; Kuzdralinski, A.; Kowalczyk, K.; Borner, A.; Nowak, M.  
464 Identification of stable reference genes for qPCR studies in common wheat (*Triticum aestivum* L.) seedlings  
465 under short-term drought stress. *Plant Methods* 2020, 16, 58, doi:10.1186/s13007-020-00601-9.

- 466 33. Lee, J.; Lee, I. Regulation and function of SOC1, a flowering pathway integrator. *Journal of Experimental*  
467 *Botany* 2010, 61, 2247-2254, doi:10.1093/jxb/erq098.
- 468 34. Carmona, M.J.; Cubas, P.; Martínez-Zapater, J.M. VFL, the grapevine FLORICAULA/LEAFY ortholog, is  
469 expressed in meristematic regions independently of their fate. *Plant Physiology* 2002, 130, 68-77.
- 470 35. Li-Mallet, A.; Rabot, A.; Geny, L. Factors controlling inflorescence primordia formation of grapevine: their  
471 role in latent bud fruitfulness? A review. *Botany* 2016, 94, 147-163.
- 472 36. Daminato, M.; Masiero, S.; Resentini, F.; Lovisetto, A.; Casadoro, G. Characterization of TM8, a MADS-box  
473 gene expressed in tomato flowers. *BMC Plant Biology* 2014, 14, 319, doi:10.1186/s12870-014-0319-y.
- 474 37. Bogs, J.; Jaffe, F.W.; Takos, A.M.; Walker, A.R.; Robinson, S.P. The grapevine transcription factor  
475 VvMYBPA1 regulates proanthocyanidin synthesis during fruit development. *Plant Physiology* 2007, 143,  
476 1347-1361, doi:10.1104/pp.106.093203.
- 477 38. Koyama, K.; Numata, M.; Nakajima, I.; Goto-Yamamoto, N.; Matsumura, H.; Tanaka, N. Functional  
478 characterization of a new grapevine MYB transcription factor and regulation of proanthocyanidin  
479 biosynthesis in grapes. *Journal of Experimental Botany* 2014, 65, 4433-4449, doi:10.1093/jxb/eru213.
- 480 39. Wong, D.C.J.; Schlechter, R.; Vannozzi, A.; Holl, J.; Hmam, I.; Bogs, J.; Tornielli, G.B.; Castellarin, S.D.;  
481 Matus, J.T. A systems-oriented analysis of the grapevine R2R3-MYB transcription factor family uncovers  
482 new insights into the regulation of stilbene accumulation. *DNA Research* 2016, 23, 451-466,  
483 doi:10.1093/dnares/dsw028.
- 484 40. Vannozzi, A.; Wong, D.C.J.; Holl, J.; Hmam, I.; Matus, J.T.; Bogs, J.; Ziegler, T.; Dry, I.; Barcaccia, G.;  
485 Lucchin, M. Combinatorial Regulation of Stilbene Synthase Genes by WRKY and MYB Transcription  
486 Factors in Grapevine (*Vitis vinifera* L.). *Plant and Cell Physiology* 2018, 59, 1043-1059,  
487 doi:10.1093/pcp/pcy045.
- 488 41. Parage, C.; Tavares, R.; Rety, S.; Baltenweck-Guyot, R.; Poutaraud, A.; Renault, L.; Heintz, D.; Lugan, R.;  
489 Marais, G.A.; Aubourg, S., et al. Structural, functional, and evolutionary analysis of the unusually large  
490 stilbene synthase gene family in grapevine. *Plant Physiology* 2012, 160, 1407-1419,  
491 doi:10.1104/pp.112.202705.
- 492 42. Yang, Y.; Zhang, L.; Chen, P.; Liang, T.; Li, X.; Liu, H. UV-B photoreceptor UVR8 interacts with  
493 MYB73/MYB77 to regulate auxin responses and lateral root development. *EMBO Journal* 2019, 39, e101928,  
494 doi:10.15252/embj.2019101928.
- 495 43. Chen, J.; Nolan, T.M.; Ye, H.; Zhang, M.; Tong, H.; Xin, P.; Chu, J.; Chu, C.; Li, Z.; Yin, Y. Arabidopsis  
496 WRKY46, WRKY54, and WRKY70 Transcription Factors Are Involved in Brassinosteroid-Regulated Plant  
497 Growth and Drought Responses. *The Plant Cell* 2017, 29, 1425-1439, doi:10.1105/tpc.17.00364.
- 498 44. Hernandez, L.D.; Vierling, E. Expression of Low Molecular Weight Heat-Shock Proteins under Field  
499 Conditions. *Plant Physiol* 1993, 101, 1209-1216, doi:10.1104/pp.101.4.1209.
- 500 45. Lindquist, S. The heat-shock response. *Annual Review Biochemistry* 1986, 55, 1151-1191,  
501 doi:10.1146/annurev.bi.55.070186.005443.
- 502 46. Burke, J.J.; Hatfield, J.L.; Klein, R.R.; Mullet, J.E. Accumulation of heat shock proteins in field-grown cotton.  
503 *Plant Physiology* 1985, 78, 394-398, doi:10.1104/pp.78.2.394.
- 504 47. Hu, W.; Hu, G.; Han, B. Genome-wide survey and expression profiling of heat shock proteins and heat  
505 shock factors revealed overlapped and stress specific response under abiotic stresses in rice. *Plant Science*  
506 2009, 176, 583-590, doi:10.1016/j.plantsci.2009.01.016.
- 507 48. Swindell, W.R.; Huebner, M.; Weber, A.P. Transcriptional profiling of Arabidopsis heat shock proteins and  
508 transcription factors reveals extensive overlap between heat and non-heat stress response pathways. *BMC*  
509 *Genomics* 2007, 8, 125, doi:10.1186/1471-2164-8-125.
- 510 49. Jaillon, O.; Aury, J.M.; Noel, B.; Policriti, A.; Clepet, C.; Casagrande, A.; Choisne, N.; Aubourg, S.; Vitulo,  
511 N.; Jubin, C., et al. The grapevine genome sequence suggests ancestral hexaploidization in major  
512 angiosperm phyla. *Nature* 2007, 449, 463-467, doi:10.1038/nature06148.
- 513 50. Dobin, A.; Davis, C.A.; Schlesinger, F.; Drenkow, J.; Zaleski, C.; Jha, S.; Batut, P.; Chaisson, M.; Gingeras,  
514 T.R. STAR: ultrafast universal RNA-seq aligner. *Bioinformatics* 2013, 29, 15-21.
- 515 51. Haak, M.; Vinke, S.; Keller, W.; Droste, J.; Rückert, C.; Kalinowski, J.; Pucker, B. High Quality de Novo  
516 Transcriptome Assembly of *Croton tiglium*. *Frontiers in Molecular Biosciences* 2018, 5, 62.
- 517 52. Liao, Y.; Smyth, G.K.; Shi, W. featureCounts: an efficient general purpose program for assigning sequence  
518 reads to genomic features. *Bioinformatics* 2014, 30, 923-930, doi:10.1093/bioinformatics/btt656.

- 519 53. Vitulo, N.; Forcato, C.; Carpinelli, E.C.; Telatin, A.; Campagna, D.; D'Angelo, M.; Zimbello, R.; Corso, M.;  
520 Vannozzi, A.; Bonghi, C., et al. A deep survey of alternative splicing in grape reveals changes in the splicing  
521 machinery related to tissue, stress condition and genotype. *BMC Plant Biology* 2014, 14, 99.
- 522 54. Barrett, P.; Hunter, J.; Miller, J.T.; Hsu, J.-C.; Greenfield, P. matplotlib – A Portable Python Plotting Package.  
523 In *Astronomical Data Analysis Software and Systems XIV ASP Conference Series, Proceedings of the*  
524 *Conference held 24-27 October, 2004 in Pasadena, California, USA*, Shopbell, P., Britton, M., Ebert, R., Eds.  
525 *Astronomical Society of the Pacific: San Francisco, 2005; Vol. 347, pp. 91-95.*
- 526 55. Guo, C.; Guo, R.; Xu, X.; Gao, M.; Li, X.; Song, J.; Zheng, Y.; Wang, X. Evolution and expression analysis of  
527 the grape (*Vitis vinifera* L.) WRKY gene family. *Journal of Experimental Botany* 2014, 65, 1513-1528,  
528 doi:10.1093/jxb/eru007.  
529  
530



© 2020 by the authors. Submitted for possible open access publication under the terms and conditions of the Creative Commons Attribution (CC BY) license (<http://creativecommons.org/licenses/by/4.0/>).

531